

analysis, using published tables of angles for  $\beta\text{-tin}$ .<sup>42</sup> The four-fold symmetry of the pattern served to eliminate the (100) and (010) orientations, which would, if present, make a contribution to the shift of opposite sign from the (001) orientation. In the eight films examined, the (001) pole was always found between 6 and 30° from the normal to the foil, with some clustering at about 20°. The average value was  $\theta=21^\circ$  with an rms deviation of 7.4°. This indicates that the (001)

<sup>42</sup> S. A. Bradford and R. W. Vieth, *Trans. Met. Soc. AIME* **236**, 232 (1966), and references cited therein.

plane is nearly the plane of the foil, but the possibility that some nearby plane, such as the (112) plane, is actually the preferred plane would have to be examined in a definitive study. For the purposes of the present experiments, the quadrupole asymmetry was calculated from the angular distribution to be  $-\Delta|$  (0.20±0.04), using also Eq. (3) and the angular intensity ratios for  $|m|$  of  $\frac{1}{2}$  and  $\frac{3}{2}$ . The uncertainty given is somewhat larger than the observed rms deviation in view of the fact that it was impractical to sample the entire area of the foil.

## Zeeman Effect in the Absorption Spectra of Trivalent Ytterbium Ions in Different Site Symmetries in Calcium Fluoride

J. KIRTON AND A. M. WHITE

*Royal Radar Establishment, Malvern, Worcestershire, England*

(Received 30 September 1968)

The Zeeman effect has been observed in the optical spectra of  $\text{Yb}^{3+}$  ions in different sites in  $\text{CaF}_2$ . All but one of the correlations between ESR and optical spectra, reported by Kirton and McLaughlan, have been checked and confirmed, and the upper-state  $g$  values have been determined. Ambiguity in the interpretation of the rhombic spectra has been eliminated, and we have shown with 90% confidence that the upper-state splitting of  $\text{Yb}^{3+}$  in cubic sites is greater than 18.3  $\text{cm}^{-1}$ .

### 1. INTRODUCTION

A RECENT study<sup>1</sup> of the  $\text{CaF}_2:\text{Yb}^{3+}$  system resulted in an attempted correlation between the optical and electron-spin-resonance (ESR) absorption spectra of  $\text{Yb}^{3+}$  ions in different site symmetries. This correlation was based on a number of measurements of specially prepared samples containing different relative concentrations of the various sites. It was not found possible to distinguish between two of the rhombic spectra (labelled  $R_1$  and  $R_2$ ) and, in every case, it was necessary to assume that sites giving observable ESR signals also gave observable optical absorption and vice versa. A much more satisfactory method of correlation is to compare the  $g$  values of the ESR lines with those of the optical lines measured in a Zeeman effect experiment. Using the latter technique, we have confirmed all but one ( $R_3$ ) of the correlations made in Ref. 1, have obtained excited state  $g$  values, and have removed the ambiguity about the rhombic spectra,  $R_1$  and  $R_2$ .

### 2. APPARATUS

All the Zeeman patterns described in this work were observed with the Poynting vector of the incident light normal to the steady magnetic field. The absorption of the samples was examined using a tungsten filament source and a single-beam Jarrell Ash 3.4-m spectrograph

operating mainly in first order. During initial surveys, a liquid-nitrogen-cooled Mullard 150 CVP photomultiplier was used for detection and the signals, after dc amplification, were recorded on a strip chart.

For precise wavelength measurements, the spectra were photographed on Kodak Type 1-M plates. Although maximum sensitivity in the region between 9200 Å and 9800 Å was obtained by using ammonia hypersensitization as recommended by the makers, it was found that the loss in sensitivity resulting from hypersensitization with triethanolamine was less important than the improvement in signal-to-noise ratio which was a consequence of the reduction in background. The spectra were photographed using an input spectral slit width of 0.25  $\text{cm}^{-1}$ , the half widths of the sharpest absorption lines being about 0.5  $\text{cm}^{-1}$ . The samples were usually cooled by mounting them on the cold fingers of either liquid-nitrogen or liquid-helium Dewars, although in selected cases, the samples were immersed in liquid helium. Samples were oriented in the magnetic field using the {111} cleavage planes of  $\text{CaF}_2$  and a 70.6° vee groove cut in a copper attachment to the Dewar cold finger. Magnetic fields were obtained from a Varian 15-in. electromagnet with 'Fieldial' control. The dimensions of the liquid-helium Dewar imposed a minimum pole gap of 2½ in. for which the maximum field was about 22 kG. Fields up to about 32 kG were obtained across a 1-in. gap when liquid-nitrogen sample cooling was employed. Although the

<sup>1</sup> J. Kirton and S. D. McLaughlan, *Phys. Rev.* **155**, 279 (1967).

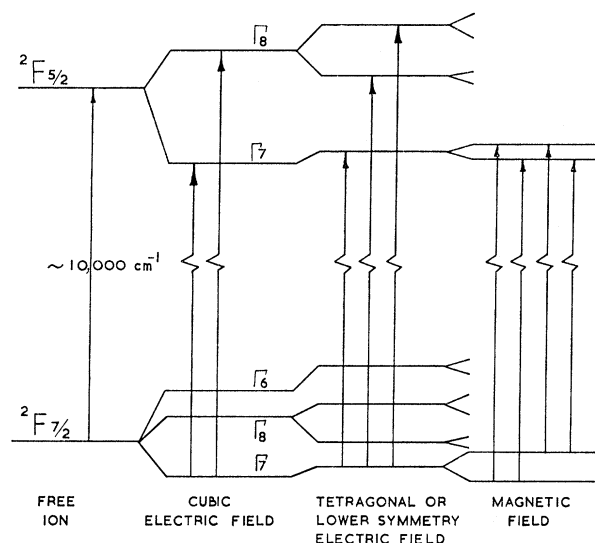


FIG. 1. Energy levels of  $\text{Yb}^{3+}$  in electric and magnetic fields.

control unit gave a nominal  $\pm 1\%$  field-setting accuracy, the fields were checked using a Varian F-8 fluxmeter and a Hewlett-Packard Type 5246L electronic counter.

Measurements were made on the photographic plates using a Hilger-Jaco L.90 comparator-microphotometer. The instrument was maintained at  $\pm 1^\circ\text{C}$  in the same air conditioned room which housed the spectrograph, and the 'working volume' was insulated from draughts. Stable readings were obtained after a 24-h warmup. The carriage position was measured on a dial gauge which could be read to  $\pm 1 \mu$  and which was calibrated in a Michelson interferometer in terms of the helium-neon gas laser wavelength. The plate was calibrated using the emission lines from low-pressure discharge lamps containing Xe, Ar, Kr, and Ne.

The samples used were the same as in the previous work and have already been described in Ref. 1.

### 3. OPTICAL SPECTRUM OF $\text{CaF}_2:\text{Yb}^{3+}$

The  $4f^{13}$  configuration of the free  $\text{Yb}^{3+}$  ion gives rise to one term  $^2F$ , which is split by spin-orbit coupling into a level  $^2F_{5/2}$   $10\,000 \text{ cm}^{-1}$  above the ground level  $^2F_{7/2}$ .

TABLE I. The expected number of Zeeman components in unpolarized spectra due to  $\text{Yb}^{3+}$  in different sites in  $\text{CaF}_2$  with the magnetic field parallel to different crystal directions. The unperturbed line is taken to be a transition between two doublets.

Site symmetry	Magnetic field direction			
	[100]	[110]	[111]	Arbitrary
Cubic	4	4	4	4
Tetragonal	8	8	4	12
Trigonal	4	8	8	16
Rhombic ( $z \parallel [110]$ and $x$ not $\parallel [100]$ e.g., $R_1$ or $R_2$ )	8	16	12	48

(Fig. 1). In a crystalline electric field having cubic symmetry, the  $^2F_{7/2}$  ground manifold breaks up into  $\Gamma_6$ ,  $\Gamma_7$  doublets and a  $\Gamma_8$  quartet, the  $\Gamma_7$  doublet being lowest in energy. The  $^2F_{5/2}$  manifold splits into a  $\Gamma_8$  quartet above a  $\Gamma_7$  doublet. In crystalline fields having tetragonal or lower symmetry, the  $\Gamma_8$  quartets are further split so that the ground manifold consists of four doublets and the  $^2F_{5/2}$  of three doublets.

### 4. ZEEMAN EFFECT FOR $\text{Yb}^{3+}$ IONS IN DIFFERENT SITE SYMMETRIES IN $\text{CaF}_2$

With the exception of the cubic case which we will consider in more detail later, there will, in general, be a number of  $\text{Yb}^{3+}$  ions in sites which are equivalent but in which the symmetry axis or axes make different angles with some fixed direction in space. For example, there will be three equivalent tetragonal sites corresponding to the symmetry axis being along the [100], [010], and [001] directions. All three sites will give rise to identical energy level diagrams and, therefore, the associated optical transitions will all be at the same frequency. Furthermore, even though each one of the sites will react differently to polarized light, the separate responses will combine to give no net anisotropy. However, if the material is placed in a magnetic field, the different equivalent sites can become nonequivalent. In the tetragonal site example, a magnetic field along the [100] direction will give Zeeman splittings equal to  $g_{\parallel}\beta H$  for sites with their axes parallel to [100] and equal to  $g_{\perp}\beta H$  for the two groups of sites with axes along [010] and [001]. For the usual doublet to doublet transitions, the Zeeman spectrum for each site will consist of four absorption lines (Fig. 1) which are usually all allowed in unpolarized light. In general, and ignoring polarization effects, for a nonspecial sample orientation and for doublet-to-doublet zero-field transitions, cubic sites will give four Zeeman lines, tetragonal sites twelve, trigonal

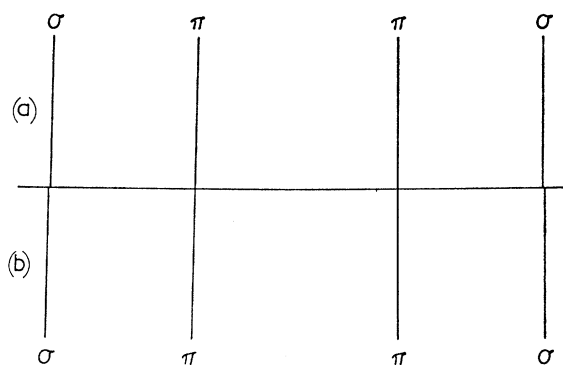


FIG. 2. Zeeman absorption spectrum of the line at  $9629.8 \text{ \AA}$ . (a) Spectrum observed at  $20 \text{ kG}$  and  $4.2^\circ\text{K}$ . (b) Spectrum calculated for magnetic dipole transition between  $\Gamma_7$  doublets of  $\text{Yb}^{3+}$  in cubic sites with  $g(J=\frac{7}{2}, \Gamma_7)=3.443$  and  $g(J=\frac{5}{2}, \Gamma_7)=-1.443$ . [ $\pi$  and  $\sigma$  refer to situations where  $\mathbf{E}$  of the incident radiation is, respectively, parallel to and perpendicular to the steady magnetic field.]

sites sixteen, and rhombic sites up to 48. A summary of what happens in general and special directions is given in Table I.

## 5. OBSERVED SPECTRA

### A. Cubic Spectrum

With liquid-nitrogen cooling and a transverse field of 27 kG it was found that the optical absorption line at 9629.8 Å in a type-C sample<sup>1</sup> was split into four components of approximately equal intensity. Changes in sample orientation left this pattern unchanged which confirmed that the centers responsible had cubic symmetry and that the terminal state was  $|J=\frac{5}{2}, \Gamma_7\rangle$  and not  $|J=\frac{5}{2}, \Gamma_8\rangle$  which would have been anisotropic. The predicted  $g$  value for the  $\Gamma_7$  doublet is  $-10/7$  (for  $J, J_z$  quantization) minus a small correction of the same order as the departure of the ground  $\Gamma_7$   $g$  value from the value  $24/7$ .<sup>2</sup> Thus, the expected upper-state  $g$  value is  $-1.443$ . Knowing this, we can construct an expected 20-kG spectrum which we have shown in Fig. 2 together with the spectrum observed at 4.2°K. The agreement is to within the experimental error. The ground-state  $g$  value was  $3.43 \pm 0.01$  at 20 kG and 4.2°K which is within experimental error of the 1.2°K ESR value of  $3.443 \pm 0.002$  obtained at 1.9 kG.

Failure to observe the  $|J=\frac{7}{2}, \Gamma_7\rangle$  to  $|J=\frac{5}{2}, \Gamma_8\rangle$  transition prevented Kirton and McLaughlan from estimating the  $\Gamma_7$ - $\Gamma_8$  splitting ( $\Delta$ ) in the upper manifold. However, a small enough  $\Gamma_7$ - $\Gamma_8$  splitting would show up in the Zeeman experiment as a nonlinearity in the  $\Gamma_7$   $g$  value as a function of magnetic field. Clearly, the best method would be to use an ESR technique as mentioned

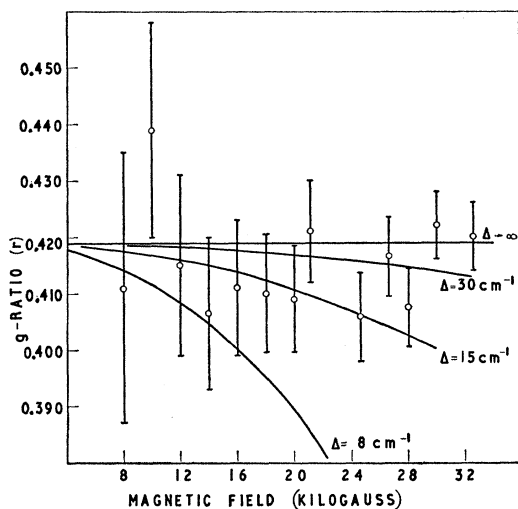


FIG. 3. Variation of the ratio of cubic  $\Gamma_7$   $g$  values as a function of magnetic field applied parallel to the  $[100]$  direction. The experimental error of  $0.12/H$  is indicated by the error bars. The curves are the computed solutions of the Hamiltonian [Eq. (1)].

<sup>2</sup> See, for example, E. S. Sabisky and C. H. Anderson, Phys. Rev. 148, 194 (1967).

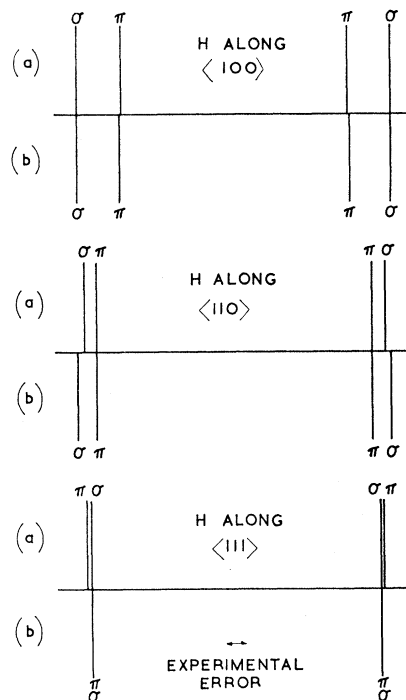


FIG. 4. Zeeman absorption spectra of the line at 9685.2 Å. The observed spectra (a) are labelled  $\pi$  and  $\sigma$  according to the convention used in Fig. 1. Identifying the various components as in Table II and using the  $g$  values of Table III the spectra (b) were calculated, using the same labels and omitting the  $\Delta\mu = \pm 1$  components.

below, but since this was not available to us, we pushed the accuracy of the optical  $g$ -value determination as far as we were able. Baker *et al.*<sup>3</sup> have placed the  $|J=\frac{7}{2}, \Gamma_8\rangle$  level at  $\sim 600 \text{ cm}^{-1}$  above the  $\Gamma_7$  ground level so non-linearity is not expected in our measurements of the ground  $\Gamma_7$   $g$  value below 100 kG. By taking this  $g$  value as constant with field, we were able to eliminate most of the possible effect of photographic emulsion distortion by simply measuring the ratio ( $r$ ) of the ground-state and upper-state splittings. The experimental values of this ratio have been plotted versus magnetic field in Fig. 3. Also shown in the figure is the variation in  $r$  with field for different values of  $\Delta$ , obtained by computing

TABLE II. Observed values of  $\delta/\beta H$  for different magnetic field orientations.  $\delta$  is the observed splitting of the line at 9685.2 Å.

Field direction	$\delta/\beta H$	Polarization	Identification
$[100]$	3.813	$\pi$	$g_{11}(\frac{5}{2}) - g_{11}(\frac{3}{2})^a$
$[100]$	5.253	$\sigma$	$g_{1}(\frac{7}{2}) - g_{1}(\frac{5}{2})$
$[110]$	4.606	$\pi$	$g_{110}(\frac{5}{2}) - g_{110}(\frac{3}{2})$
$[110]$	5.024	$\sigma$	$g_{1}(\frac{7}{2}) - g_{1}(\frac{5}{2})$
$[111]$	4.965	$\pi$	$g_{111}(\frac{5}{2}) - g_{111}(\frac{3}{2})$
$[111]$	4.830	$\sigma$	$g_{111}(\frac{7}{2}) - g_{111}(\frac{5}{2})$

<sup>a</sup>  $g(5/2)$ , the  $g$  value of the  $J=5/2$  doublet, is negative.

<sup>3</sup> J. M. Baker, W. B. J. Blake, and G. M. Copland, Phys. Letters 26A, 504 (1968).

TABLE III. Summary of optical and ESR  $g$  values for  $\text{Yb}^{3+}$  in different sites in  $\text{CaF}_2$ .

Site symmetry	ESR ground-state $g$ values <sup>a</sup>			Wavelength of zero-field line ( $\text{\AA}$ )	Ground-state optical $g$ values			Upper-state optical $g$ values		
	$g_x$	$g_y$	$g_z$		$g_x$	$g_y$	$g_z$	$g_x$	$g_y$	$g_z$
Cubic	$g_{\text{isotropic}} = 3.443 \pm 0.002$			9629.8	$g_{\text{isotropic}} = 3.43 \pm 0.01$			$g_{\text{isotropic}} = -1.42 \pm 0.03$		
Tetragonal	$3.802 \pm 0.005$		$2.412 \pm 0.003$	9685.2	b			$-1.47 \pm 0.05^e$	$-1.41 \pm 0.05^e$	
Trigonal $T_1$	$4.389 \pm 0.004$		$1.323 \pm 0.001$	9815.0	$4.38 \pm 0.03$		$1.33 \pm 0.03$	$2.36 \pm 0.03$	$-0.57 \pm 0.03$	
Trigonal $T_2$	$4.389 \pm 0.004$		$1.421 \pm 0.001$	9749.1	$4.40 \pm 0.04$		$1.44 \pm 0.04$	$2.39 \pm 0.04$	$-0.57 \pm 0.04$	
Trigonal $T_3$	$4.291 \pm 0.005^d$		$1.516 \pm 0.002$	9824.4	$4.34 \pm 0.03$		$1.49 \pm 0.03$	$2.19 \pm 0.03$	$0.36 \pm 0.03$	
Rhombic $R_1$	$6.99 \pm 0.01$	$1.355 \pm 0.002$	$1.094 \pm 0.002$	9736.6	$6.95^e$	$1.41$	$1.11$	$3.71$	$0.83$	$0.32$
Rhombic $R_2$	$7.24 \pm 0.01$	$0.992 \pm 0.002$	$0.957 \pm 0.002$	9764.7	$7.18$	$1.22$	$1.12$	$3.81$	$0.75$	$0.47$
Rhombic $R_3$	$3.4 \pm 0.2^f$	$1.241 \pm 0.002$	$1.096 \pm 0.002$	...	...	...	...	...	...	...
Rhombic $R_4$	$6.45 \pm 0.02$	$2.175 \pm 0.002$	$1.667 \pm 0.002$	...	...	...	...	...	...	...
Rhombic $R_5$	$3.926 \pm 0.005$	$3.289 \pm 0.005$	$3.102 \pm 0.005$	9636.8	...	...	...	...	...	...

<sup>a</sup> Reference 1.

<sup>b</sup> Not determined in experiment.

<sup>c</sup> Calculated from experiment using ESR data for ground-state  $g$  values.

<sup>d</sup> This value is different to that reported in Refs. 1 and 8. S. D. McLaughlan has informed us of the corrected value which we have given in this table.

<sup>e</sup> The error is not known due to the uncertain effect of overlapping of the spectra.

<sup>f</sup> Calculated from information given privately by S. D. McLaughlan.

the eigenvalues of the Hamiltonian

$$\mathcal{H} = b_4/60(O_4^0 + 5O_4^4) + \frac{1}{2}g_N\beta H\{2lJ_x + (m-in)J_+ + (m+in)J_-\} \quad (1)$$

acting on the manifold of states with  $J = \frac{5}{2}$ .  $b_4$  is a crystal-field parameter,  $O_4^0$  and  $O_4^4$  are Stevens' Operator equivalents, and  $l$ ,  $m$ , and  $n$  are the direction cosines of the steady magnetic field with respect to the  $[100]$  crystal direction. It is clear that the  $\Gamma_7$ - $\Gamma_8$  splitting  $\Delta$  is greater than  $8 \text{ cm}^{-1}$  so that the results can be fitted to the approximate expression

$$r = r_0 - BH^2,$$

where  $r$  is the ratio at field  $H$ ,  $r_0$  at zero field, and  $B$  is equal to  $320\beta^2/147\Delta^2$ . A least-squares fit gives  $r_0 = 0.415 \pm 0.005$  and  $B = (0.01 \pm 8.58) \times 10^{-6} \text{ kG}^{-2}$ . Since the error contains most of the information, we have estimated it both theoretically and from a statistical examination of our experimental results. Both estimates agree, and we conclude that  $\Delta$  is greater than  $18.3 \text{ cm}^{-1}$  with 90% confidence.

Since the recent letter by Low<sup>4</sup> we have reexamined our spectra but have been unable to find a second cubic line corresponding to the transition  $|J = \frac{1}{2}, \Gamma_7\rangle$  to  $|J = \frac{5}{2}, \Gamma_8\rangle$  at temperatures down to  $4.2^\circ\text{K}$ . It seems worthwhile to search for ESR from the optically populated upper  $\Gamma_7$  level and carry out an ENDOR measurement of the type carried out by Baker *et al.* for the ground  $\Gamma_7$  level.

## B. Tetragonal Spectrum

The interpretation of the results on the line at  $9685.2 \text{ \AA}$  has been less satisfactory due to the absence of a number of Zeeman components. For example, if this line is indeed due to  $\text{Yb}^{3+}$  in tetragonal sites, as previously suggested,<sup>1</sup> the  $\pi$  spectrum for  $H_0 \parallel [100]$  would be expected to consist of four  $\Delta\mu = 0$  transitions,<sup>5</sup> two each from the sites with fourfold axes parallel and

perpendicular to the steady magnetic field. The  $\sigma$  spectrum would be expected to consist of four  $\Delta\mu = \pm 1$  transitions. In fact, we observed only two lines in each case which appeared to correspond to the selection rule  $\Delta\mu = 0$ , giving splittings proportional to  $g_{11}(\frac{1}{2}) + |g_{11}(\frac{5}{2})|$  and  $g_1(\frac{1}{2}) + |g_1(\frac{5}{2})|$ . Similar situations arose when the dc field was parallel to the  $[110]$  and  $[111]$  directions. By utilizing the ESR data, we were able to obtain values for the upper state  $g$  values which, subject to the above restriction and the identifications set out in Table II, gave calculated spectra close to those observed. Figure 4 displays a comparison between the observed spectra and those calculated in this manner. The upper-state  $g$  value is isotropic to within experimental error<sup>6</sup> and close to the value  $(-1.423)$  which can be obtained from an eigenvector, built from states within the  $J = \frac{5}{2}$  manifold of  $\text{Yb}^{3+}$ . The only other possible isotropic  $g$  value from such an eigenstate would be  $+1.836$ .

As the magnitudes of the upper-state  $g$  values are consistent with what would result from  $\text{Yb}^{3+}$ , we feel confident that the consistent picture we have built up on the assumption that the fundamental line is due to tetragonal  $\text{Yb}^{3+}$  sites is not a coincidence. However, we are unable to explain the absence of the  $\Delta\mu = \pm 1$  transitions.

A strictly isotropic  $g$  value would place a restriction on the crystal-field parameters, which in the notation of Weber and Bierig<sup>7</sup> is

$$b_2^0 = (55/27)(b_4^4 - b_4^0).$$

## C. Trigonal Spectra

These will be described in a separate publication, and we need only state here that the correlations reported by Kirton and McLaughlan for  $T_1$ ,  $T_2$ , and  $T_3$  have been fully confirmed. The  $g$  values are summarized in Table III.<sup>8</sup>

<sup>6</sup> Greater than the cubic case due to the increased line width.

<sup>7</sup> M. J. Weber and R. W. Bierig, Phys. Rev. **134**, 1492 (1964).

<sup>8</sup> S. D. McLaughlan and R. C. Newman, Phys. Letters **19**, 552 (1965).

<sup>4</sup> W. Low, Phys. Letters **26A**, 234 (1968).

<sup>5</sup>  $\mu$  is the crystal-field quantum number.

TABLE IV. Ground-state  $g$  values of rhombic spectra.

Wavelength of zero-field line	Optical results					ESR Center	ESR results <sup>a</sup>				
	$H\parallel[100]$		$H\parallel[111]$				$H\parallel[100]$		$H\parallel[111]$		
	$g_1$	$g_2$	$g_3$	$g_4$	$g_5$		$g_1$	$g_2$	$g_3$	$g_4$	$g_5$
9736.6 Å	1.467	4.974	1.240	5.843	5.603	$R_1$	1.408	4.996	1.208	5.967	5.538
9764.7 Å	3.383	4.670	2.137	7.079	3.578	$R_2$	3.329	4.650	2.075	7.168	3.556
						$R_3$	1.333	2.502	1.180	2.591	3.094
						$R_4$	2.175	4.711	1.852	5.414	5.414

<sup>a</sup> Calculated from Ref. 1.

#### D. Rhombic Spectra

The lines at 9736.6 Å and 9764.7 Å have been examined along [100] and [111] directions. The spectra were more complex than those described above, and the overlapping of lines sometimes gave rise to ambiguous interpretations for one particular pattern. However, only one self consistent set of  $g$  values resulted when both orientations were taken into account. In Table IV the ground-state  $g$  values predicted from ESR for these directions are compared with those observed. The overlapping of lines gave rise to an error which we have not been able to estimate so that no errors are included in the optical  $g$  values reported for the rhombic spectra. However, it is clear that the shorter wavelength line is  $R_1$  and the other line  $R_2$ . Thus, we have removed the ambiguity left in the earlier investigation and are

able to report the excited-state  $g$  values. We have computed the principal  $g$  values and these are presented in Table III. The  $g$  values observed in our chosen directions are rather insensitive to the values of  $g_\nu$  and  $g_z$ , and in consequence the values of these two parameters which give a least-squares fit carry a larger uncertainty.

#### 6. CONCLUSIONS

We have confirmed all but one of the correlations reported by Kirton and McLaughlan and have removed the ambiguity about the lines belonging to the rhombic ESR spectra  $R_1$  and  $R_2$ . We have shown with 90% confidence that the upper-state splitting of  $\text{Yb}^{3+}$  in cubic sites is greater than  $18.3 \text{ cm}^{-1}$ . Excited-state  $g$  values have been tabulated for the identified sites.

### Anomalous Population Distributions in an Optically Excited Metastable Level in $\text{CaF}_2:\text{Tm}^{2+}$

C. H. ANDERSON AND E. S. SABISKY  
*RCA Laboratories, Princeton, New Jersey 08540*  
 (Received 3 October 1968)

The population distribution among the magnetic sublevels of the metastable state of  $\text{CaF}_2:\text{Tm}^{2+}$  is shown to be strongly influenced by spin orientation memory from the ground state. This memory is dependent on the wavelength and polarization of the pump radiation, being quite strong at 5790 Å. The population is also influenced by an optical cross-relaxation or excitation transfer between neighboring ions, particularly so because the hyperfine splittings in the ground and excited states are almost identical. Also, it is shown that there is a high degree of nuclear spin orientation memory.

#### I. INTRODUCTION

THIS is the second of two papers on paramagnetic resonance in the optically excited metastable level in  $\text{CaF}_2:\text{Tm}^{2+}$ . The first paper<sup>1</sup> dealt with the measurement of the  $g$  value and hyperfine constants in the excited state and the comparison of these values with crystal-field theory. This paper is concerned with the anomalous population distributions observed in the magnetic sublevels in the excited state and their interpretation.

<sup>1</sup> E. S. Sabisky and C. H. Anderson, Phys. Rev. 148, 194 (1966).

A normal Boltzmann distribution among the magnetic sublevels of an optically excited state will be observed if the spin lattice relaxation rate between the sublevels is fast compared to the optical decay rate out of the state. However, if the normal thermalization rate is slower than the decay rate, the population distribution in the magnetic sublevels can become sensitive to other processes, which can result in very different distributions. Under the latter condition in  $\text{CaF}_2:\text{Tm}^{2+}$ , we have observed two distinct mechanisms which are important in determining the population distribution. The first is what we call spin orientation memory, which